JACS
JOURNAL OF THE AMERICAN CHEMICAL SOCIETY
pubs.acs.org/JACS
Article

Tuning Orbital Symmetry of Iridium Nitrenoid Enables Catalytic Diastereo- and Enantioselective Alkene Difunctionalizations

Suhyeon Kim, Dongwook Kim, Seung Youn Hong,* and Sukbok Chang*

Cite This: J. Am. Chem. Soc. 2021, 143, 3993−4004
Read Online
ACCESS | Metrics & More | Article Recommendations | Supporting Information

ABSTRACT: Among the central themes in synthetic chemistry is the establishment of novel strategies that usher in the development of more efficient and mild reactions and also expand the chemical space for asymmetric catalysis. Herein, we present an approach to revitalize the Cp*Ir(κ^2-LX) system as a catalyst toward alkene difunctionalizations via a nitrenoid-mediated pathway. A key strategy is tuning the orbital symmetry of the key Ir nitrenoid intermediates by ligand modification to impart the desired catalytic activity with the suppression of catalyst deactivation. On the basis of a frontier molecular orbital (FMO) analysis, we systematically engineered a new catalyst system capable of a stepwise nitrenoid transfer to allow for nucleophile incorporation. Using the catalytic protocol, a range of difunctionalized lactams can be produced in a diastereoselective manner with various nucleophiles. Mechanistic investigations revealed that the ligand plays a crucial role in both nitrenoid-delivery and stereoselectivity-determining steps. The current mechanistic platform also enabled the development of new asymmetric methods for introducing two-point chirality in (oxyalkyl)lactam products with excellent enantioselectivity.

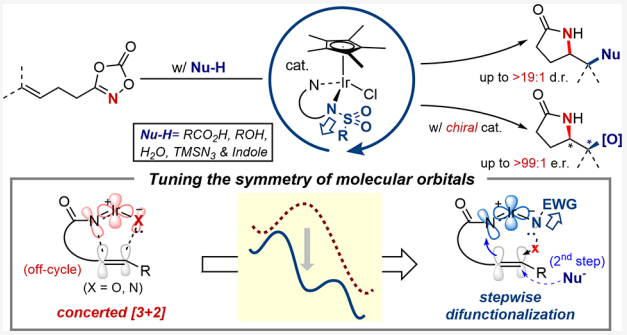

INTRODUCTION

Difunctionalization of alkenes is a versatile strategy for constructing two C(sp^3)−X bonds (X = O, N, halides, etc.) in a single operation, enabling a rapid access to molecular complexity.[1−4] Of these transformations, a procedure that installs at least one amino group is particularly attractive, as it can grant an efficient and straightforward route to valuable nitrogen-containing scaffolds from readily available olefin precursors.[5,6] While recent years have witnessed some notable strategies to design racemic alkene difunctionalizations,[7−21] the growing demands for chiral amines in the pharmaceutical industry have also fueled burgeoning interest in developing the asymmetric variants for their synthesis.[22−24]

In this context, nitrenoid transfer catalysis has attracted considerable attention since the pioneering works by Sharpless on asymmetric aminohydroxylations.[25−29] From a mechanistic standpoint, alkene difunctionalization driven by amino group transfer can be classified into two types. As depicted in Scheme 1a, a two-step approach involving aziridination of olefins and then ring opening triggered by an exogenous nucleophile is one of the most widely utilized methods in chemical synthesis.[30−41] For instance, the Schomaker[42] and Zhang[43] groups independently developed elegant ways of accessing chiral bicyclic aziridines, which are readily converted to enantioenriched heterocyclic products through additional transformations. An alternative pathway denoted as ligand participation at the bottom of Scheme 1a, where an auxiliary ligand plays an additional role as an internal nucleophile that inserts into double bonds cooperatively, has also shown great promise in their applications. Examples include the landmark achievements using Os-based catalysts[25−29,44−46] and Fe-catalyzed oxazolidinone synthesis reported by Bach,[47] Xu,[48−51] and others.[52] Despite the significant advances within these mechanistic scaffolds, the majority of the known methods rely primarily on the need for specialized nitrene precursors containing sulfone or carbamate on nitrogen.[53] However, the incorporation of an amide functionality into an alkene via a nitrenoid-mediated process remains less explored.[54−56] Especially, to our knowledge, there is currently no such method for selectively inducing the desired chirality into the organic commodities. This may be ascribed to the lack of a multifaceted system capable of (i) suppressing the Curtius-type decomposition of the key acylnitrenoid,[57,58] (ii) facilitating catalytic olefin difunctionalization, and (iii) controlling both diastereo- and enantioselectivities. Therefore, the development of another selective approach to transferring an amido group across a double bond is highly desirable.

Received: January 19, 2021
Published: March 5, 2021

https://dx.doi.org/10.1021/jacs.1c00652
J. Am. Chem. Soc. 2021, 143, 3993−4004

Scheme 1. Mechanistic Approaches to Alkene Difunctionalization via Nitrenoid Transfer

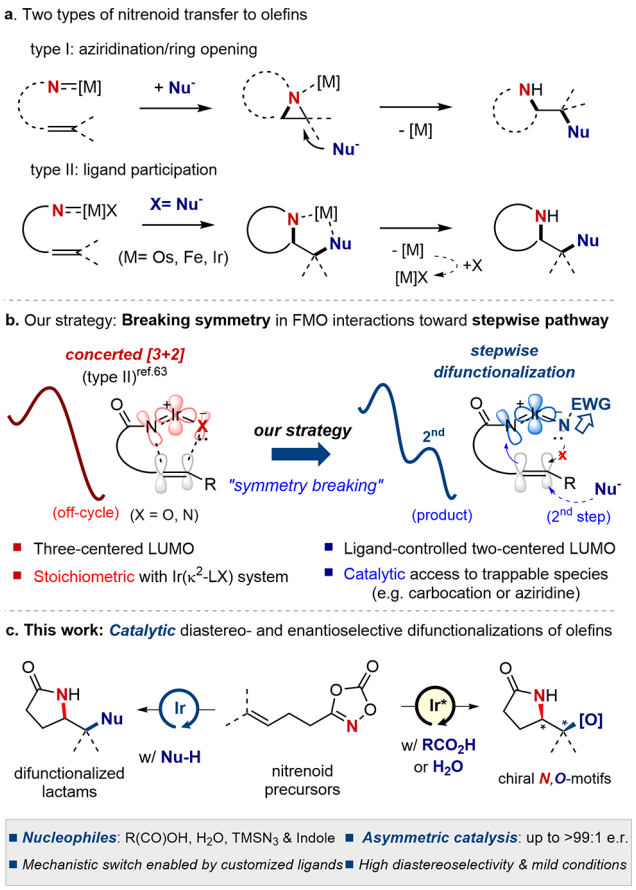

In our research program for efficient and selective C−N bond-forming reactions,[59−62] we recently demonstrated that a Cp*Ir(κ^2-LX) complex can serve as a handle for capitalizing on the dipole-like reactivity of an Ir nitrenoid toward concerted [3 + 2] cycloaddition via ligand participation (Scheme 1b, left).[63] However, this manifold has been examined exclusively in stoichiometric studies because the resultant tridentate chelate is highly robust against further transformations. In the pursuit of catalytic reactions, we envisioned that, upon modification of the ligands, the symmetry of the nitrenoid LUMO could be repurposed to break key orbital interactions for the concerted pathway, which consequently would render it stepwise (Scheme 1b, right). This newly proposed mechanistic route may allow for the catalytic generation of either carbocation or aziridine intermediates,[64] both of which will be intercepted with external trapping agents and lead to the same difunctionalized amine products of high synthetic utility.[65]

Here we present a design strategy in which the known concerted pathway can be diverted to stepwise olefin difunctionalization by tuning the orbital symmetry of the key Ir nitrenoid (Scheme 1c). On the basis of the principle established by FMO analysis, we identified that catalysts bearing a sulfonylamino group are optimal for producing a wide range of functionalized γ-lactams in a highly stereoselective manner. Mechanistic investigations revealed that the sulfone moiety in the ligand allows the *syn*-selective insertion of protic nucleophiles to lead to unprecedented high stereoselectivity. Not only can carboxylic acids be employed as a nucleophile but also alcohols, H_2O, $TMSN_3$, and indole can be used. Moreover, the extension of the current mechanistic scaffold to an asymmetric induction was successfully achieved with excellent enantioselectivity (up to >99:1 e.r.), thereby enabling the simultaneous introduction of two stereogenic centers for the production of important chiral compounds.

RESULT AND DISCUSSION

Attempts to Develop Catalytic Reactions Using Previously Employed Complexes. We previously described well-defined Cp*Ir(κ^2-LX) complexes (**Ir**) leveraging the intermediacy of a carbonyl nitrenoid toward C−H amidation reactions.[61] Moreover, the same type of complex could also be applicable for alkene difunctionalization, where an olefin-tethered substrate is transformed into ligand-participated complexes (**i**) in a stoichiometric fashion (Scheme 2a).[63]

Scheme 2. Initial Attempts to Explore Catalytic Activity

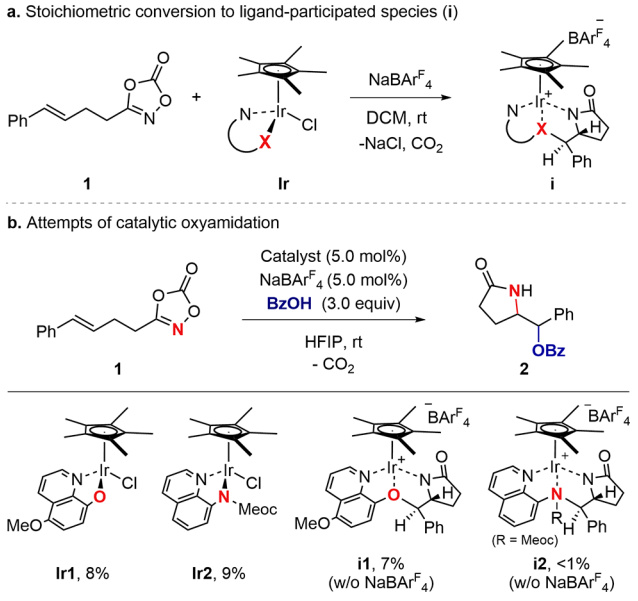

The key to success was that the postulated Ir nitrenoid has the character of an electrophilic 1,3-dipole provoked by a three-centered LUMO. Therefore, it can interact with a C═C bond via a concerted [3 + 2] cycloaddition mode. Although this mechanistic underpinning provides the foundation for the development of catalytic oxyamidation reactions by employing a distinct combination of $[Cp^{ArF}IrCl_2]_2$ and acetic acid, the Cp*Ir(κ^2-LX) system could not be utilized for the catalytic conversions. Recently, Rovis and co-workers reported a complementary method for producing identical products via an aziridination pathway.[66] Notwithstanding this precedent, there is room for improvement in the areas of nucleophiles and enantioselectivity control.

Building on our previous works and that of Rovis, we wondered whether a catalytic oxyamidation method could be developed utilizing **Ir** as a catalyst. This is based on the anticipation that the use of **Ir** would provide a general catalytic regime that incorporates a broader array of nucleophiles applicable to this transformation, making this approach synthetically more versatile. Toward this end, we initially evaluated the catalytic activity of the previously employed Ir complexes in the reaction of (γ-alkenyl)dioxazolone **1** with an oxygen nucleophile (Scheme 2b). We selected benzoic acid as

https://dx.doi.org/10.1021/jacs.1c00652
J. Am. Chem. Soc. 2021, 143, 3993−4004

a model reactant because aryl-substituted carboxylic acids were previously problematic as nucleophiles. However, **Ir1** and **Ir2**, which were known to engage in vicinal difunctionalization in our recent stoichiometric studies,[63] were found to be ineffective in affording the desired oxygenated lactam **2**. With regard to the low-yielding results, we reasoned that complexes **i** embedded in tridentate chelates would be initially generated but they remain unreacted in the subsequent desired reaction with benzoic acid, thus resulting in an off-catalytic cycle. This rationale was further supported by control experiments. For example, using preisolated **i1** or **i2** as a catalyst, only low efficiency was observed in the formation of product **2** (Scheme 2b).

Design Principle for Optimal Ligand Systems. To address the issue of such a catalyst deactivation, we envisaged devising an alternative mechanistic pathway (Scheme 3a). As

Scheme 3. Principle of Ligand Design

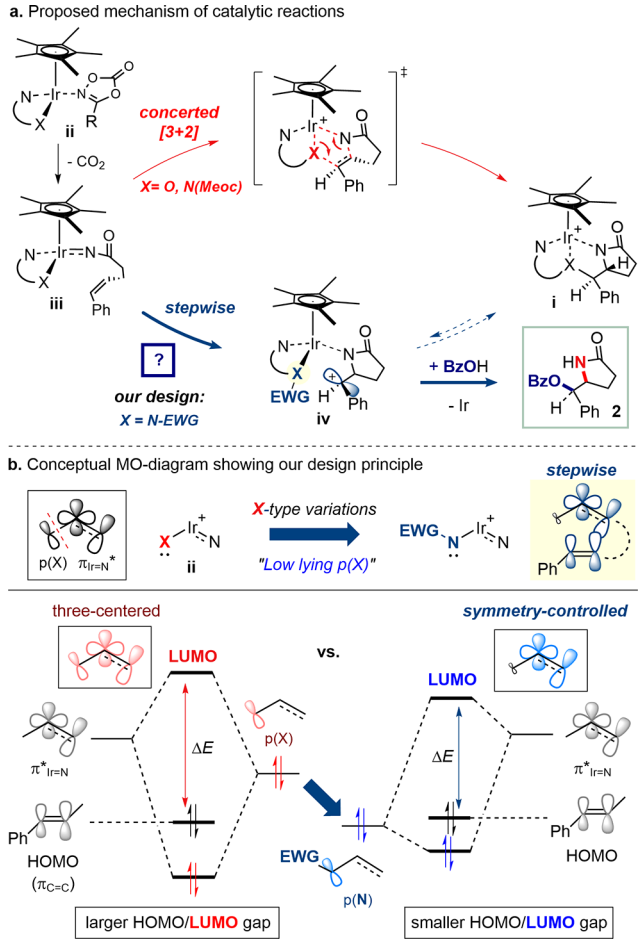

we previously proposed, the initial step in catalysis is the decarboxylation of the iridium−dioxazolone adduct **ii** to generate the postulated Ir nitrenoid **iii**. We conjectured that nitrenoid insertion into a pendant olefin can occur via either concerted [3 + 2] or stepwise pathways. While the former process leads to the aforementioned off-cycle species **i**, the latter can generate the transient carbocation **iv**, likely via electrophilic addition. The intermediate **iv** can then be engaged in a reaction with benzoic acid to outcompete an undesired nucleophilic trapping by the bidentate ligands. Finally, the desired product **2** will be formed with regeneration of the catalyst.

Given that the ligand participation of an anionic moiety (X) and thus a three-centered LUMO is a prerequisite for the concerted reaction mode,[63] we hypothesized that replacing a contact atom of X by a nitrogen substituted with an electron-withdrawing group (EWG) may engender attenuating its π-electron-donating ability by the action of the lower-lying p(X) orbital (Scheme 3b). The consequent nitrenoid would feature a symmetry-controlled shape of the LUMO consisting of predominantly d(Ir) and p(N) orbitals, which may allow for unveiling the designed stepwise process. Additionally, as the p(X) orbital is less engaged in overlap with the Ir=N bond fragment ($\pi^*_{Ir=N}$), the HOMO/LUMO gap of the corresponding nitrenoid is predicted to be smaller, thereby leading to enhanced electrophilicity.

Reaction Development. On the basis of the above qualitative MO analysis, we set out our investigations of the influence of catalyst structure on the desired oxyamidation reactivity (Table 1). We focused on 8-aminoquinoline-based ligands because their high tunability on the N substituents was anticipated to lead to the discovery of effective catalysts. First, varying the steric environment of the ligand was found to exert

Table 1. Catalyst Optimization[a]

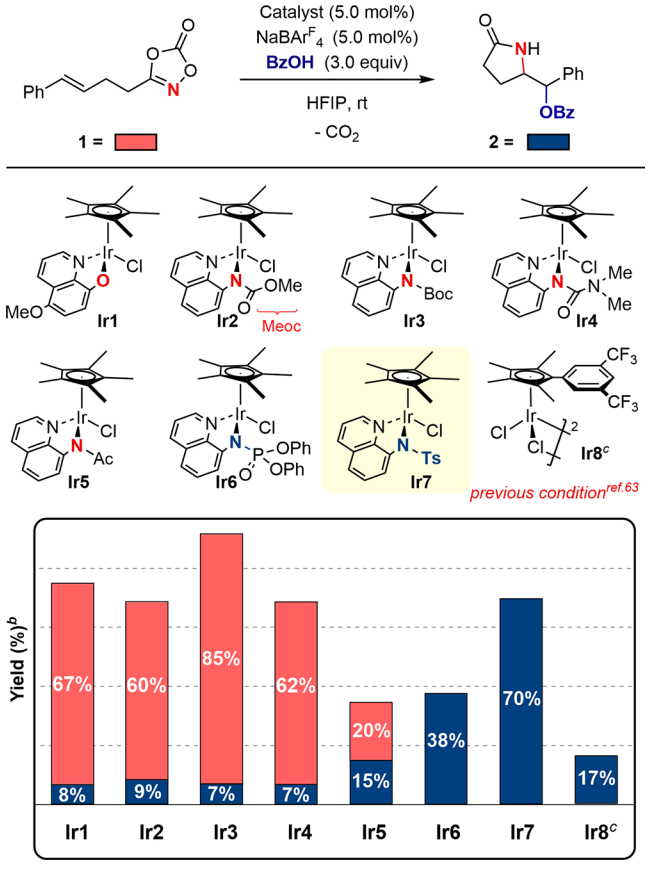

[a]Conditions unless specified otherwise: **1** (0.05 mmol), **Ir** (5.0 mol %), $NaBAr^F_4$ (5.0 mol %), and BzOH (3.0 equiv) in HFIP (0.3 mL) at rt for 12 h. Meoc = methoxycarbonyl [b]Yields were based on a ^{1}H NMR analysis of the crude reaction mixture using 1,1,2,2-tetrachloroethane as an internal standard. [c]Conditions: **1** (0.1 mmol), **Ir8** (2.5 mol %), $AgNTf_2$ (10 mol %), NaOH (40 mol %), and BzOH (1.5 equiv) in HFIP (0.3 mL) at 60 °C.

https://dx.doi.org/10.1021/jacs.1c00652
J. Am. Chem. Soc. 2021, 143, 3993−4004

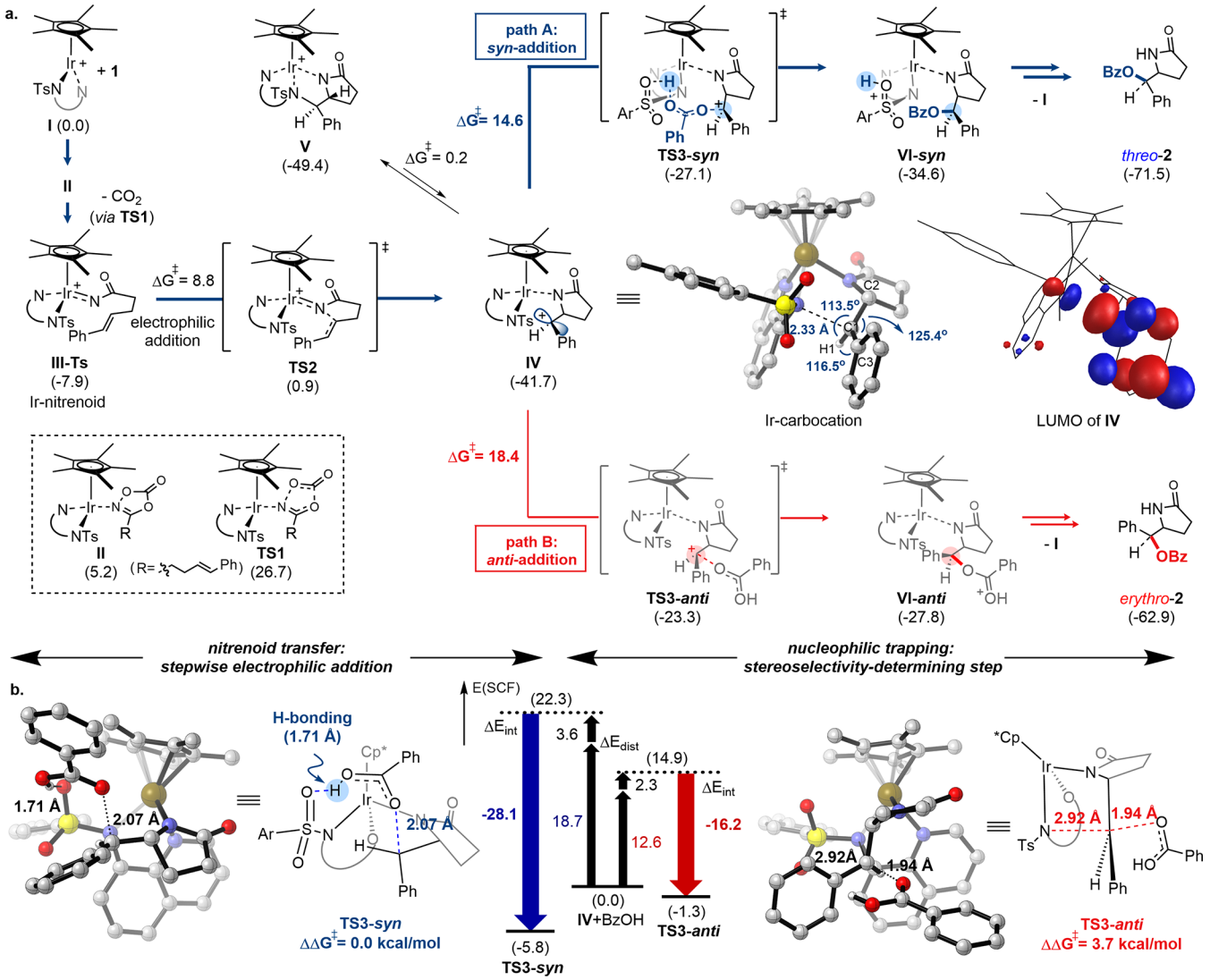

Figure 1. Computational studies: (a) reaction profiles calculated at the PCM(HFIP)-M06/SDD+6-311++G**//M06/Lanl2dz+6-31G** level of theory (Δ*G* in kcal/mol); (b) computed structures of **TS3-*syn*** and **TS3-*anti*** with the results of EDA (Δ*E* in kcal/mol).

no beneficial effects on the cyclization efficiency. For instance, when *tert*-butyloxycarbonyl (Boc, **Ir3**) and carbamoyl groups (**Ir4**) were substituted, most of the starting material (**1**) remained intact with only small amounts of the desired product (<10% of **2** each). Switching the amino protecting group to the acetyl moiety (**Ir5**) gave rise to only a marginal improvement in product yield.

As was initially hypothesized, we found that modifying the electronic properties of the catalysts was critical for the catalytic oxyamidation. The use of catalyst **Ir6** bearing a phosphorylamino group led to full consumption of **1**, albeit with low product yield (38%). Pleasingly, the *N*-sulfonyl-substituted complex **Ir7** displayed good catalytic activity at room temperature for transforming **1** into lactam **2** in high yield (70%) with excellent diastereoselectivity (>19:1 d.r.). Intriguingly, the oxyamidation took place in a *syn*-selective manner, as evidenced by the *threo*-configuration in the major isomer **2**. In terms of other reaction parameters, hexafluoro-2-propanol (HFIP) and nonafluoro-*tert*-butyl alcohol (NFTB) were the most effective solvents, whereas aprotic media such as dichloromethane (DCM) and acetonitrile led to a significant decrease in the reaction efficiency (see the Supporting Information for details). In contrast, the reaction was sluggish even at higher temperature under the previously developed conditions using **Ir8**, which highlights the superior catalytic performance of our currently developed system.

Computational Modeling. For a better understanding of how catalyst **Ir7** can efficiently mediate the catalytic oxyamidation with excellent *syn*-selectivity, the energy landscape of the reaction progress was evaluated by density functional theory (DFT) calculations and the results are summarized in Figure 1. The reaction commences with the binding of dioxazolone **1** to a coordinatively unsaturated 16-electron complex (**I**) generated *in situ* by chloride abstraction from the neutral precursor **Ir7**.[67] The resulting adduct **II** can liberate a molecule of carbon dioxide, affording the singlet Ir nitrenoid species **III-Ts** located at −7.9 kcal/mol. For this step traversing the transition state **TS1**, an energy of 26.7 kcal/mol was calculated to be required. Unlike the previously proposed concerted pathway,[63] our computations show that **III-Ts** undergoes an electrophilic addition across the double bond via **TS2** with a barrier of 8.8 kcal/mol to yield the intermediate **IV**. The carbocationic character of **IV** was embodied in the nearly planar geometry at the benzylic C1

https://dx.doi.org/10.1021/jacs.1c00652
J. Am. Chem. Soc. 2021, 143, 3993−4004

center and its empty p orbital, as witnessed by the LUMO. While an intramolecular nucleophilic addition of the nitrogen atom (N2) on the ligand can produce ligand-participated species **V**, only a low kinetic hurdle (0.2 kcal/mol from **IV** and 7.9 kcal/mol from **V**) suggests that the interconversion between **IV** and **V** is facile, thus pushing further productive pathways.

An analysis of molecular orbitals in the bond-forming process provided an explanation for the origin of the distinctive working mode of **III-Ts**. For a direct comparison, the complex **Ir2** was selected as a control group to represent ineffective systems. As seen in Figure 2a, the nitrenoid **III-Meoc** derived

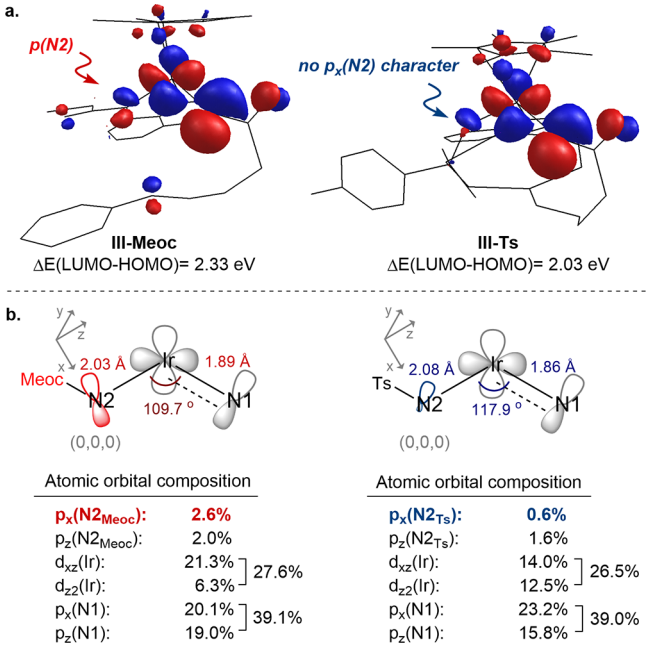

Figure 2. (a) Computed LUMOs of **III-Meoc** and **III-Ts** with their HOMO/LUMO energy gaps (isovalue: 0.05). (b) Population of atomic orbitals calculated using the M06 functional in the ADF package.

from **Ir2** has a LUMO that shows a three-center system, reminiscent of ozone or nitrous oxide.[68] In contrast, the LUMO of **III-Ts** derived from **Ir7** implicates the antibonding coupling ($\pi^*_{Ir=N}$) between the d(Ir) and p(N1) orbitals (Figure 2a, right). The most conspicuous aspect is that the contribution of the p(N2) orbital is relatively small mainly due to poor orbital overlap between $\pi^*_{Ir=N}$ and p(N2), as described in Scheme 2b. In addition, irrespective of **III-Meoc** or **III-Ts**, the HOMO was calculated to reside predominantly at the π-bonding orbital of an alkenyl moiety (see the Supporting Information for details). Remarkably, the energy gap between the HOMO and LUMO in **III-Ts** derived from **Ir7** is 2.03 eV, which is the smallest value in comparison with those of other less effective Cp*Ir(*N,N'*-chelate) complexes **Ir2**–**Ir6** (see the Supporting Information for details), in support of accentuating the electrophilicity of **III-Ts** induced by the sulfonyl group.

To further validate the above interpretation quantitatively, we carried out Amsterdam density functional (ADF) calculation (Figure 2b).[69−71] For a Cartesian coordinate, we chose the N2 atom in **III** as a center point and an Ir−N2 bond as standard settings for denoting the *z* axis. In cases where LUMOs of **III-Meoc** and **III-Ts** are partitioned into atomic orbitals, there are no significant differences between the two species in the populations of d(Ir) and p(N1). In contrast, the composition of p_x(N2) is decreased more than 4-fold from 2.6% in **III-Meoc** to 0.6% in **III-Ts**. This negligible p_x(N2) contribution in **III-Ts** results in the orbital symmetry behaving like a two-centered LUMO. Overall, the nitrenoid unit in **III-Ts** interacts with only one carbon center (C2) of the intramolecular alkenyl moiety without any incorporation of the sulfonylamino group to access the intermediacy of carbocation **IV**.

The Origin of Diastereoselectivity. To account for the excellent stereoselectivity observed in the addition of benzoic acid using **Ir7** (Table 1), we considered plausible mechanistic scenarios in the selectivity-determining step (Figure 1a). Quantum chemical calculations revealed that carbocation **IV** will react with benzoic acid by traversing either **TS3-*syn*** or **TS3-*anti***, which leads to different stereochemical outcomes. As shown in path A of Figure 1a, the *threo*-configured product **2** is formed via the *syn*-selective route passing through the product-bound species **VI-*syn*** with a $\Delta G^{\ddagger}$ value of 14.6 kcal/mol. On the other hand, the transition state **TS3-*anti*** for the production of the *erythro*-isomer is 3.7 kcal/mol higher in energy than **TS3-*syn***. These theoretical values are fully consistent with the selectivity trend observed in our experiments (>19/1 *syn*/*anti*, Table 1).

Careful inspection of each diastereomeric transition state underlines the importance of the sulfone group in nucleophilic substitution as well as the initial nitrenoid transfer stages. As visualized in Figure 1b, the energetically more favorable **TS3-*syn*** has a H-bond between the sulfonyl oxygen atom of the catalyst and the O−H hydrogen of benzoic acid with a distance of 1.71 Å. In contrast, the minor transition state **TS3-*anti*** lacks such secondary interactions, implying that the customized bidentate ligand in **Ir7** may be crucial for selectively promoting the *syn*-addition pathway.

The energy difference between the two competing pathways was further scrutinized by an energy decomposition analysis (EDA)[72] as summarized in the middle of Figure 1b. With the reactant state as the starting point, the intermediate **IV** must adopt the distorted geometry found in the transition states to react with benzoic acid. The total distortion energies (ΔE_{dis}) of **TS3-*syn*** and **TS3-*anti*** were calculated to be 22.3 and 14.9 kcal/mol, respectively. Meanwhile, the stronger interaction in **TS3-*syn*** relative to **TS3-*anti*** appears to be 11.9 kcal/mol higher in energy, and it can compensate for the higher distortion energy, thus leading to a more favorable *syn*-addition. The final electronic energy difference of 4.5 kcal/mol between the two transition states is well reflected in the calculated kinetic preference for **TS3-*syn*** ($\Delta\Delta G^{\ddagger}$ = 3.7 kcal/mol). When these results are taken together, we conclude that the unique behavior of the sulfonyl moiety makes the difference in the electronic interaction in the transition states, which is a key component for the observed *syn*-selectivity.

Reaction Scope of Ir-Catalyzed Olefin Difunctionalization. Having identified the critical role of the *N*-sulfonyl group of **Ir7** during catalysis, we next investigated the general applicability of the current working system by testing a range of olefin-tethered substrates (Table 2). As robust nitrenoid precursors, all of the dioxazolones we examined were conveniently prepared from the corresponding carboxylic acids in two synthetic steps with high yields in general.[73,74] (*E*)-(Aryl)alkenyl dioxazolones with electronic perturbations

https://dx.doi.org/10.1021/jacs.1c00652
J. Am. Chem. Soc. 2021, 143, 3993−4004

Table 2. Reaction Scope in the Alkene Difunctionalizations[a]

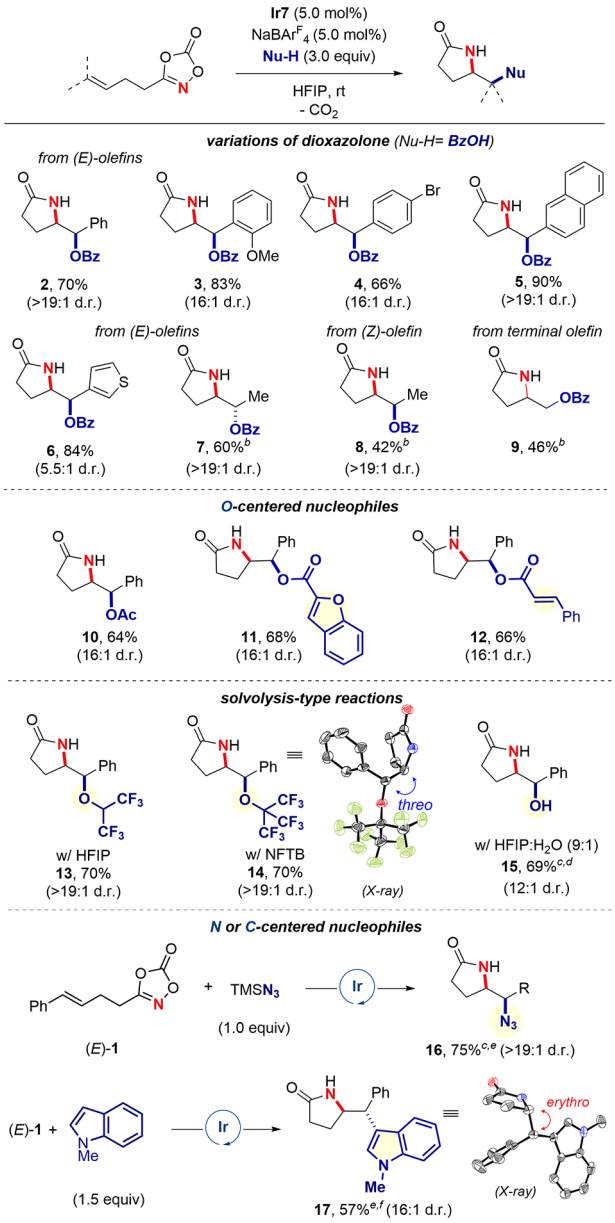

[a]Reaction conditions unless specified otherwise: (*E*)-Substrate (0.2 mmol), **Ir7** (5.0 mol %), NaBAr$^F_4$ (5.0 mol %) and nucleophiles in HFIP at 25 °C for 12 h. [b]Run at 60 °C. [c]**Ir7** (10 mol %) and NaBAr$^F_4$ (10 mol %) were used. [d]NMR yield. [e]NFTB solvent was used instead of HFIP.

on the phenyl group were smoothly converted to the corresponding cyclized products (**2**−**4**) in good to high yields and with excellent diastereoselectivities. Naphthalene (**5**) and thiophene (**6**) were compatible with the present protocol. However, a (*Z*)-isomeric substrate ((*Z*)-**1**) provided a mixture of two diastereomeric products (2.3:1, eq 1), presumably due

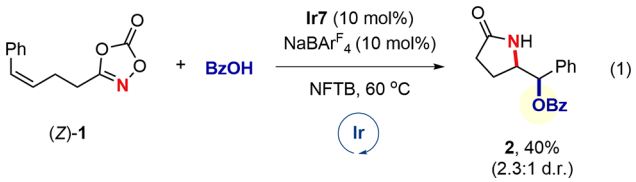

(1)

to the fleeting nature of the rotatable carbocation intermediate **IV** in equilibrium with **V**, as shown in Figure 1a, thus leading to only partial convergence via a minimal C−C bond rotation (see the Supporting Information for details).[64] The cyclization of substrates containing (*E*)- and (*Z*)-alkyl-substituted internal olefins gave the expected products **7** and **8**, respectively, with excellent *anti*-selectivities (>19:1 d.r.) regardless of the olefin geometry. In these cases, the oxyamidation may proceed via a cascade aziridination and ring opening, as recently proposed by the Rovis group.[66] This may be attributed to the lack of driving force for accessing the corresponding aliphatic carbocation without resonance stabilization, thereby leading to the aziridine-involved pathway. Moreover, a terminal olefinic substrate derived from 4-pentenoic acid was successfully cyclized to yield γ-(oxymethyl)-2-pyrrolidone **9**, albeit with moderate efficiency.[75]

Motivated by the mechanistic insights into the involvement of readily trappable carbocationic species, we surmised that the repertoire of the alkene difunctionalizations could be expanded by altering the external nucleophiles. Not only benzoic acid but also alkyl (**10**), heteroaryl (**11**), and alkenyl carboxylic acids (**12**) were found to be suitable oxygen sources to afford a suite of lactam-substituted esters with high stereoselectivities. In the absence of an external reagent, alcoholic solvents such as HFIP (**13**) and NFTB (**14**) can function as reactive oxygen donors themselves to permit solvolysis-type reactions. The stereochemistry of one major diastereomeric product, **14**, was confirmed as *threo* by a crystallographic analysis to suggest that a cognate interaction between the ligand and nucleophile is valid for the addition of alcohols. More importantly, an unprotected OH group can also be directly incorporated by using water as a nucleophile when a cosolvent system (HFIP/H_2O 9/1) was employed. With a higher catalyst loading, the synthetically useful hydroxyl NH-lactam **15** can be synthesized with high *syn*-selectivity.

After surveying the scope of oxyamidations, we subsequently checked the feasibility of other classes of nucleophiles. The installation of two orthogonal nitrogen units at the pendant alkene can be attained by coupling with $TMSN_3$ as an azido source. This procedure provided a route to unsymmetrical 1,2-diamine derivatives (**16**) for potential use in synthesis, coordination, and click chemistry.[76−78] Moreover, *N*-methylindole acted as a coupling partner toward the carboamidation reaction to give the indole-incorporated product **17** with high diastereoselectivity. It should be mentioned that an *erythro*-product was obtained as a major diastereoisomer in this case. It can be rationalized that such a carbon-centered nucleophile cannot engage in a H-bonding interaction with the ligand, thus obligating the *anti*-addition pathway.[79]

Development of Asymmetric Reactions. Chiral γ-lactams, particularly those that contain an α′-oxyalkyl group at the γ-position, are prevalent in both naturally occurring products[80,81] and clinical candidates[82−85] (Scheme 4a). Despite their significant contributions to synthetic and medicinal chemistry, an efficient and modular method for these privileged scaffolds has lagged behind. One commonly used procedure involves multistep derivatizations starting from pyroglutamic acid or its derivatives.[86−89] However, the high cost and limited accessibility of such chiral pool molecules impede further applications.[90] In this context, we put forward a new retrosynthetic disconnection approach that involves an enantioselective oxyamidation for constructing chiral γ-(α′-oxyalkyl)lactams from readily available carboxylic acids

https://dx.doi.org/10.1021/jacs.1c00652
J. Am. Chem. Soc. 2021, 143, 3993−4004

Scheme 4. Chiral γ-(α′-Oxyalkyl)lactam of High Synthetic Value

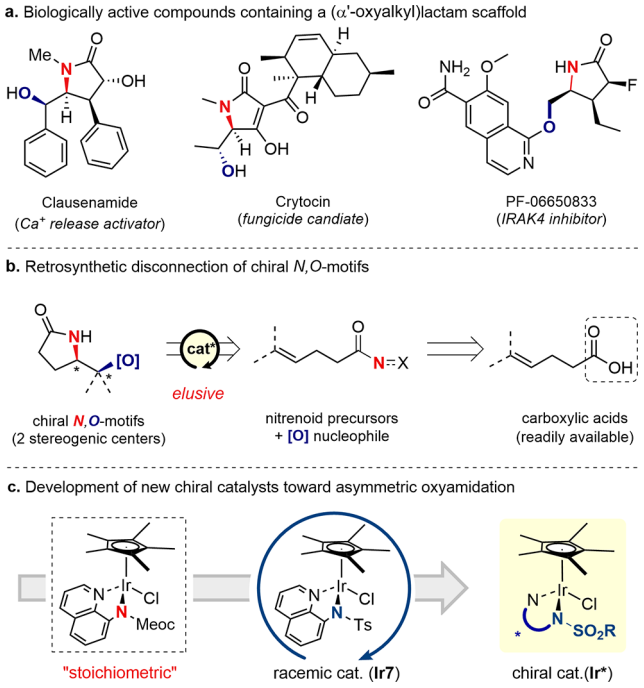

(Scheme 4b). From a synthetic point of view, the difficulty lies in setting two-point chirality, where both C(sp^3)−N and C(sp^3)−O bonds must be newly forged in a diastereo- and enantioselective fashion. To surmount the selectivity challenge, we envisaged taking advantage of our current mechanistic platform as a basis for advancing a new chiral catalyst (Scheme 4c).

Seeking to develop a tailored catalyst for the asymmetric induction, we paid special attention to chiral *N*-sulfonyl diamine derivatives as potential ligands on the basis of the following considerations: (i) Ir complexes with such diamine scaffolds, originally developed by Noyori for asymmetric hydrogenation reactions,[91] have been proven by us to be effective not only for generating the related Ir nitrenoid but also for discriminating prochiral C(sp^3)−H bonds during nitrenoid delivery[92] and (ii) the S-bound oxygen atom in the sulfonyl ligand is predicted to impart the ability to define another stereochemistry arising from nucleophile addition.

We accordingly investigated the reactivity and selectivity toward the asymmetric oxyamidation by subjecting 5 mol % of chiral catalysts in the reaction of substrate **1** with acetic acid (Table 3). Using the diamine catalyst **Ir*1**, it being optimal for the asymmetric C(sp^3)−H insertion chemistry as shown in our previous work,[92] we commenced our study for the envisioned asymmetric olefin difuctionalization (entry 1). The expected product (**2**) was indeed produced with promising stereoselectivity (12:1 d.r. and 81:19 e.r.), albeit in low yield. A diphenylethylenediamine catalyst (**Ir*2**) also displayed parallel reactivity in comparison to that of **Ir*1** (entry 2). Encouraged by these initial results, we extensively derivatized the diamine catalysts to evaluate the influence of stereoelectronic properties on their effectiveness. While variations at the *N*-sulfonyl aryl moieties gave only a marginal change (entries 3−5), catalyst **Ir*6** bearing two electron-withdrawing groups (the trifluoromethyl group, CF_3) showed slightly improved stereoselectivity (entry 6). On the other hand, an additional

Table 3. Evaluation of Chiral Catalysts

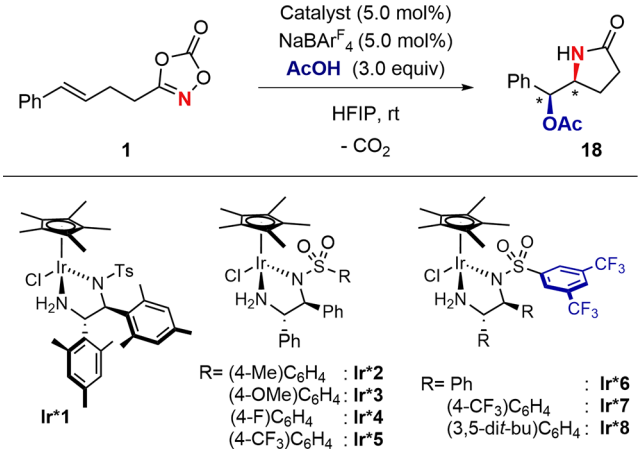

entry	catalyst	yield of **18** (%)[a]	d.r.[b]	e.r.[c]
1	**Ir*1**	26	12:1	81:19
2	**Ir*2**	27	13:1	83:17
3	**Ir*3**	34	10:1	84:16
4	**Ir*4**	34	16:1	84:16
5	**Ir*5**	35	17:1	84:16
6	**Ir*6**	37	18:1	89:11
7	**Ir*7**	24	11:1	85:15
8	**Ir*8**	44	>19:1	94:6
9[d]	**Ir*8**	47	15:1	99:1
10[e]	**Ir*8**	63	12:1	99:1

[a]^{1}H NMR yield using 1,1,2,2-tetrachloroethane as an internal standard. [b]Diastereoisomeric ratio determined by ^{1}H NMR spectra of the crude mixture. [c]Enantiomeric ratio determined by chiral high-performance liquid chromatography (HPLC). [d]NFTB solvent (0.6 mL) was employed in lieu of HFIP. [e]fNFTB solvent (0.1 mL) was used.

installation of the CF_3 unit to phenyl moieties at the ethylene backbone (**Ir*7**) did not increase the reaction efficiency (entry 7). To our delight, the deliberate modification of the catalyst to effectuate steric crowding in the secondary coordination sphere (**Ir*8**) was translocated into a satisfactory level of enantioselectivity (entry 8). Subsequently, screening additional reaction parameters revealed that the NFTB solvent was more suited for the desired oxyamidation to give chiral **2** in 99:1 e.r. (entry 9) and the product yield was further enhanced at higher concentration (entry 10).

The catalyst **Ir*8** adopts salient structural features that further provide insight into the proposed role of the sulfonylamino group in the nucleophilic addition step. As illustrated in Figure 3, the crystal structure of **Ir*8** is well-organized through multiple noncovalent interactions. For instance, one of the sulfonyl oxygen atoms is in close contact with a hydrogen atom of one methyl group at the Cp* ring with an O···H bond distance of 2.327 Å. Moreover, another oxygen atom of the sulfonyl moiety is engaged in an intermolecular hydrogen bond with NH donors of another catalyst to create a H-bonding network in the cluster where the NH···O distance is observed to be 2.589 Å. These observations implicate that the S-bound oxygen atoms can work in the capacity of H-bonding acceptors. In fact, such a behavior of the sulfone moiety was previously known to operate in homogeneous catalysis and often be a key strategy for accelerating the reaction kinetics[93] and also exploring a new redox catalysis upon a dynamic coordination.[94]

https://dx.doi.org/10.1021/jacs.1c00652
J. Am. Chem. Soc. 2021, 143, 3993−4004

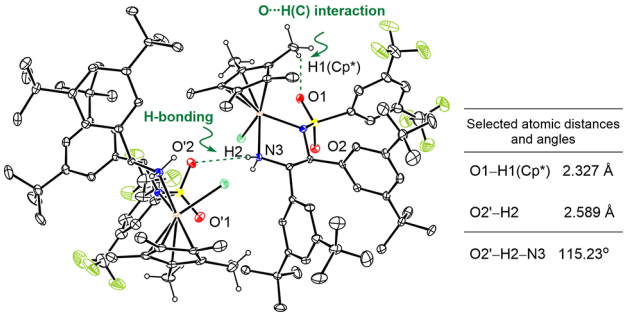

Figure 3. Solid-state structure of **Ir*8** with selected data. The BAr^F_4 anion and unimportant H atoms are omitted for clarity.

Generality of Asymmetric Oxyamidation. With the optimal chiral catalyst **Ir*8** in hand, the substrate scope of asymmetric difunctionalization was explored next (Table 4). When (*E*)-olefins substituted with an aryl moiety were subjected to the standard conditions, the reactions were highly diastereo- and enantioselective (**18**–**21**). No significant erosion of stereoselectivities was observed when an aromatic carboxylic acid was employed in lieu of acetic acid (**18** versus **19**). The absolute configuration of the enantiomeric product **20** (>99:1 e.r.) was assigned to be (*S*,*S*) by an X-ray crystallographic analysis to reveal that the oxygen nucleophile was added in a *syn*-selective manner as predicted. Substrates having a dialkyl internal olefin underwent the desired asymmetric oxyamidation to afford γ-(α′-oxyalkyl)lactam products still with excellent enantioselectivies (**22**–**24**). In these cases, the oxygen and nitrogen were exclusively added to the opposite sides (*anti*) of the C=C double bond leading to *erythro*-configured products. In addition, a substrate prepared from (*Z*)-hex-4-enoic acid was successfully transformed into an aliphatic *threo*-lactam with a diastereomeric ratio of >19:1 but with diminished enantioselectivity (**25**). Significantly, the oxyamidation of trisubstituted olefinic substrates was also facile with excellent enantioselectivity (**26** and **27**), although the diastereoselectivity was rather low in the former case. Chirality transfer from the catalyst to a sterically unbiased terminal olefin was also possible, albeit with moderate enantioselectivity (**28**).

By expanding the scope of nucleophiles to benzoic acid having one chloride atom, the stereochemistry of the corresponding product **29** was unambiguously assigned to be in an (*S*,*R*) configuration. Isobutyric acid was feasible as an oxygen source (**30**). Moreover, naturally occurring carboxylic acids such as fenbufen (**31**) and lithocholic acid (**32**) were also applicable to synthesize more complex chiral molecules. It is noteworthy that the latter case, where no alcohol-incorporated side product was detected in the reaction mixture, demonstrates the high chemoselectivity in our current system.

In addition, a solvolysis-type difunctionalization of alkenyl dioxazolone took place in a highly stereoselective fashion when HFIP or NFTB was employed as the solvent in the absence of external nucleophiles (**33** and **34**, Scheme 5). The virtue of the current protocol was further demonstrated by achieving a hydroxyamidation using water as a practical OH source as well as a chloride abstractor[95] to streamline enantioselective access to vicinal N(H),O(H) motifs (**35**) with contiguous chiral centers, which are a sought-after feature in complex molecule synthesis.

Table 4. Substrate Scope of Asymmetric Oxyamidation[a]

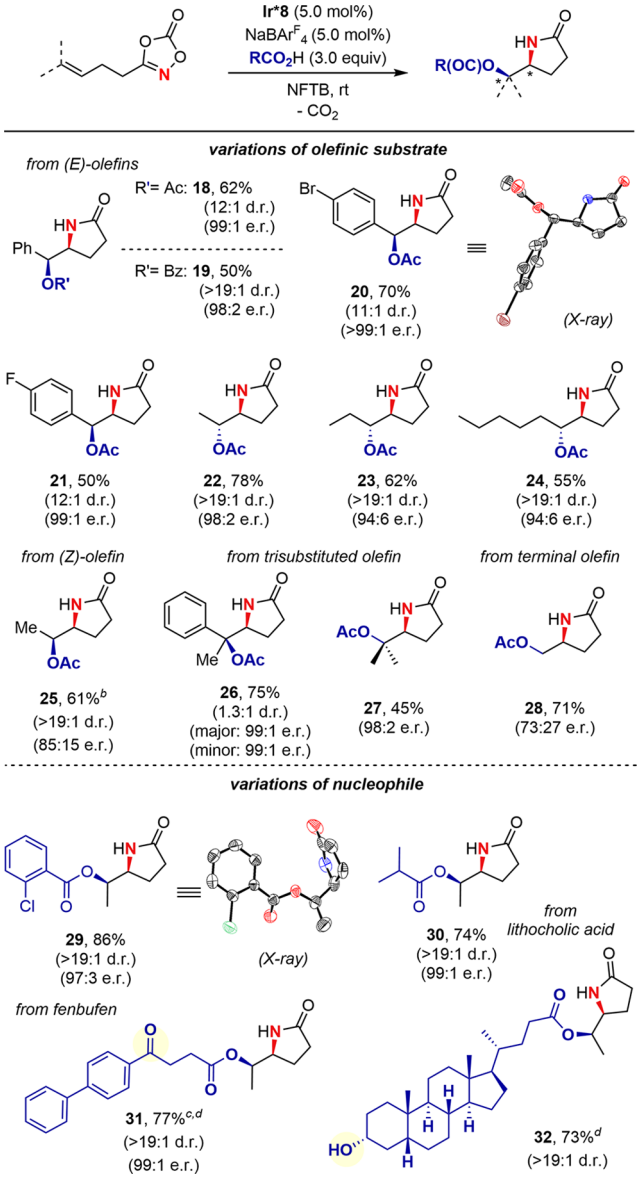

[a]Conditions unless specified otherwise: substrate (0.2 mmol), **Ir*8** (5.0 mol %), $NaBAr^F_4$ (5.0 mol %), and carboxylic acid (0.6 mmol) in NFTB (0.2 mL) at 25 °C for 12 h. [b]Catalyst **Ir*6** was used instead of **Ir*8**. [c]Under diluted conditions (0.4 mL of NFTB). [d]1.5 equiv of carboxylic acid was used.

CONCLUSION

Our initial working hypothesis that the orbital symmetry of metal nitrenoids can be tailored to suit catalytic olefin difunctionalization has been successfully implemented. Pinpointing the prototypical reaction mode of the Ir nitrenoid to give a ligand-participating off-cycle pathway, we were able to build up an alternative design for new chemically innocent ligands. Upon evaluation of a series of Ir(LX) complexes with modification of the X-chelating unit, the sulfone-based catalyst system was shown to be the most effective for accessing either carbocation or aziridine intermediates, depending on the olefin substituents. Aryl substituents on the double bond allow a catalytic access to the carbocation intermediate, whereas the reactions of (alkyl)alkenyl substrates proceed via a stepwise process involving the aziridine. We observed that both

https://dx.doi.org/10.1021/jacs.1c00652
J. Am. Chem. Soc. 2021, 143, 3993−4004

Scheme 5. Asymmetric Solvolysis Reactions

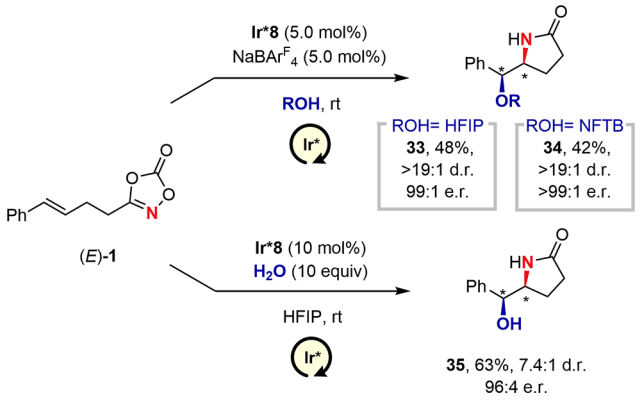

transient intermediates smoothly reacted with nucleophiles, leading to the desired oxyamidated products with unprecedented high stereoselectivities. In addition to FMO analysis, the computations revealed that the sulfone-based ligand is crucially responsible for both tuning the orbital symmetry in the nitrenoid transfer step and also assisting in the addition of nucleophiles via an attractive interaction. Benefiting from the present catalytic protocol, we have succeeded in broadening the entries of nucleophiles such as water, azide, and indole in addition to carboxylic acids and therefore achieving stereoselective oxy-, azido-, and carboamidations. The mechanism-driven design logic could be harnessed to engineer a challenging asymmetric transformation. We have indeed developed a new catalyst system bearing a customized chiral diamine backbone to allow the concurrent generation of two stereogenic centers from alkenyl dioxazolones. The method can provide, for the first time, modular access to chiral γ-(α'-oxyalkyl)lactams with excellent diastereo- and enantioselectivities of up to >99:1 e.r.. We anticipate that the design principles applied in this study will inspire further developments for exploring fundamentally distinct mechanistic modes in functional group transfer catalysis.

■ ASSOCIATED CONTENT

Supporting Information

The Supporting Information is available free of charge at https://pubs.acs.org/doi/10.1021/jacs.1c00652.

Experimental procedures, NMR spectra for the products, X-ray crystallographic data, and computational details (PDF)

Accession Codes

CCDC 2055432−2055438 contain the supplementary crystallographic data for this paper. These data can be obtained free of charge via www.ccdc.cam.ac.uk/data_request/cif, or by emailing data_request@ccdc.cam.ac.uk, or by contacting The Cambridge Crystallographic Data Centre, 12 Union Road, Cambridge CB2 1EZ, UK; fax: +44 1223 336033.

■ AUTHOR INFORMATION

Corresponding Authors

Seung Youn Hong − *Center for Catalytic Hydrocarbon Functionalization, Institute for Basic Science (IBS), Daejeon 34141, Korea; Department of Chemistry, Korea Advanced Institute of Science and Technology (KAIST), Daejeon 34141, Korea;* orcid.org/0000-0003-0113-5276; Email: hsy141@kaist.ac.kr

Sukbok Chang − *Center for Catalytic Hydrocarbon Functionalization, Institute for Basic Science (IBS), Daejeon 34141, Korea; Department of Chemistry, Korea Advanced Institute of Science and Technology (KAIST), Daejeon 34141, Korea;* orcid.org/0000-0001-9069-0946; Email: sbchang@kaist.ac.kr

Authors

Suhyeon Kim − *Department of Chemistry, Korea Advanced Institute of Science and Technology (KAIST), Daejeon 34141, Korea; Center for Catalytic Hydrocarbon Functionalization, Institute for Basic Science (IBS), Daejeon 34141, Korea;* orcid.org/0000-0001-7618-1854

Dongwook Kim − *Center for Catalytic Hydrocarbon Functionalization, Institute for Basic Science (IBS), Daejeon 34141, Korea; Department of Chemistry, Korea Advanced Institute of Science and Technology (KAIST), Daejeon 34141, Korea;* orcid.org/0000-0003-4432-371X

Complete contact information is available at: https://pubs.acs.org/10.1021/jacs.1c00652

Notes

The authors declare no competing financial interest.

■ ACKNOWLEDGMENTS

This article is dedicated to Professor Kyo Han Ahn for his honorable retirement with great contributions in chemistry and inspiring mentorship. This research was supported by the Institute for Basic Science (IBS-R010-D1) in Korea. We thank Mr. Joon Heo (KAIST) for helpful discussions. Single-crystal X-ray diffraction experiments with synchrotron radiation were performed at the BL2DSMC beamline at Pohang Accelerator Laboratory.

■ REFERENCES

(1) Shimizu, Y.; Kanai, M. Recent progress in copper-catalyzed difunctionalization of unactivated carboncarbon multiple bonds. *Tetrahedron Lett.* **2014**, *55*, 3727−3737.

(2) Garlets, Z. J.; White, D. R.; Wolfe, J. P. Recent Developments in Pd(0)-catalyzed Alkene Carboheterofunctionalization Reactions. *Asian J. Org. Chem.* **2017**, *6*, 636−653.

(3) Lan, X.-W.; Wang, N.-X.; Xing, Y. Recent Advances in Radical Difunctionalization of Simple Alkenes. *Eur. J. Org. Chem.* **2017**, *2017*, 5821−5851.

(4) Sauer, G. S.; Lin, S. An Electrocatalytic Approach to the Radical Difunctionalization of Alkenes. *ACS Catal.* **2018**, *8*, 5175−5187.

(5) Trowbridge, A.; Walton, S. M.; Gaunt, M. J. New Strategies for the Transition-Metal Catalyzed Synthesis of Aliphatic Amines. *Chem. Rev.* **2020**, *120*, 2613−2692.

(6) Park, Y.; Kim, Y.; Chang, S. Transition Metal-Catalyzed C−H Amination: Scope, Mechanism, and Applications. *Chem. Rev.* **2017**, *117*, 9247−9301.

(7) Wu, T.; Yin, G.; Liu, G. Palladium-Catalyzed Intramolecular Aminofluorination of Unactivated Alkenes. *J. Am. Chem. Soc.* **2009**, *131*, 16354−16355.

(8) Zhao, B.; Peng, X.; Zhu, Y.; Ramirez, T. A.; Cornwall, R. G.; Shi, Y. Cu(I)-Catalyzed Diamination of Conjugated Dienes. Complementary Regioselectivity from Two Distinct Mechanistic Pathways Involving Cu(II) and Cu(III) Species. *J. Am. Chem. Soc.* **2011**, *133*, 20890−20900.

(9) Ingalls, E. L.; Sibbald, P. A.; Kaminsky, W.; Michael, F. E. Enantioselective Palladium-Catalyzed Diamination of Alkenes Using *N*-Fluorobenzenesulfonimide. *J. Am. Chem. Soc.* **2013**, *135*, 8854−8856.

(10) Miyazaki, Y.; Ohta, N.; Semba, K.; Nakao, Y. Intramolecular Aminocyanation of Alkenes by Cooperative Palladium/Boron Catalysis. *J. Am. Chem. Soc.* **2014**, *136*, 3732−3735.
(11) Faulkner, A.; Scott, J. S.; Bower, J. F. An Umpolung Approach to Alkene Carboamination: Palladium Catalyzed 1,2-Amino-Acylation, -Carboxylation, -Arylation, -Vinylation, and -Alkynylation. *J. Am. Chem. Soc.* **2015**, *137*, 7224−7230.
(12) Rajbongshi, K. K.; Saikia, I.; Chanu, L. D.; Roy, S.; Phukan, P. A Metal-Free Protocol for Aminofunctionalization of Olefins Using $TsNBr_2$. *J. Org. Chem.* **2016**, *81*, 5423−5432.
(13) Fu, N.; Sauer, G. S.; Saha, A.; Loo, A.; Lin, S. Metal-catalyzed electrochemical diazidation of alkenes. *Science* **2017**, *357*, 575−579.
(14) Liu, Y.-Y.; Yang, X.-H.; Song, R.-J.; Luo, S.; Li, J.-H. Oxidative 1,2-carboamination of alkenes with alkyl nitriles and amines toward γ-amino alkyl nitriles. *Nat. Commun.* **2017**, *8*, 14720.
(15) Shen, K.; Wang, Q. Copper-Catalyzed Alkene Aminoazidation as a Rapid Entry to 1,2-Diamines and Installation of an Azide Reporter onto Azahetereocycles. *J. Am. Chem. Soc.* **2017**, *139*, 13110−13116.
(16) Nakafuku, K. M.; Fosu, S. C.; Nagib, D. A. Catalytic Alkene Difunctionalization via Imidate Radicals. *J. Am. Chem. Soc.* **2018**, *140*, 11202−11205.
(17) Siu, J. C.; Sauer, G. S.; Saha, A.; Macey, R. L.; Fu, N.; Chauviré, T.; Lancaster, K. M.; Lin, S. Electrochemical Azidooxygenation of Alkenes Mediated by a TEMPO−N_3 Charge-Transfer Complex. *J. Am. Chem. Soc.* **2018**, *140*, 12511−12520.
(18) Li, Y.; Liang, Y.; Dong, J.; Deng, Y.; Zhao, C.; Su, Z.; Guan, W.; Bi, X.; Liu, Q.; Fu, J. Directed Copper-Catalyzed Intermolecular Aminative Difunctionalization of Unactivated Alkenes. *J. Am. Chem. Soc.* **2019**, *141*, 18475−18485.
(19) Ren, X.; Guo, Q.; Chen, J.; Xie, H.; Xu, Q.; Lu, Z. Visible-Light Promoted Distereodivergent Intramolecular Oxyamidation of Alkenes. *Chem. - Eur. J.* **2016**, *22*, 18695−18699.
(20) Wardrop, D. J.; Bowen, E. G.; Forslund, R. E.; Sussman, A. D.; Weerasekera, S. L. Intramolecular Oxamidation of Unsaturated O-Alkyl Hydroxamates: A Remarkably Versatile Entry to Hydroxy Lactams. *J. Am. Chem. Soc.* **2010**, *132*, 1188−1189.
(21) Makai, S.; Falk, E.; Morandi, B. Direct Synthesis of Unprotected 2-Azidoamines from Alkenes via an Iron-Catalyzed Difunctionalization Reaction. *J. Am. Chem. Soc.* **2020**, *142*, 21548−21555.
(22) Tao, Z.; Gilbert, B. B.; Denmark, S. E. Catalytic, Enantioselective syn-Diamination of Alkenes. *J. Am. Chem. Soc.* **2019**, *141*, 19161−19170.
(23) Muñiz, K.; Barreiro, L.; Romero, R. M.; Martínez, C. Catalytic Asymmetric Diamination of Styrenes. *J. Am. Chem. Soc.* **2017**, *139*, 4354−4357.
(24) Liwosz, T. W.; Chemler, S. R. Copper-Catalyzed Enantioselective Intramolecular Alkene Amination/Intermolecular Heck-Type Coupling Cascade. *J. Am. Chem. Soc.* **2012**, *134*, 2020−2023.
(25) Sharpless, K. B.; Patrick, D. W.; Truesdale, L. K.; Biller, S. A. New reaction. Stereospecific vicinal oxyamination of olefins by alkyl imido osmium compounds. *J. Am. Chem. Soc.* **1975**, *97*, 2305−2307.
(26) Herranz, E.; Biller, S. A.; Sharpless, K. B. Osmium-catalyzed vicinal oxyamination of olefins by *N*-chloro-*N*-argentocarbamates. *J. Am. Chem. Soc.* **1978**, *100*, 3596−3598.
(27) Li, G.; Angert, H. H.; Sharpless, K. B. *N*-Halocarbamate Salts Lead to More Efficient Catalytic Asymmetric Aminohydroxylation. *Angew. Chem., Int. Ed. Engl.* **1996**, *35*, 2813−2817.
(28) Rudolph, J.; Sennhenn, P. C.; Vlaar, C. P.; Sharpless, K. B. Smaller Substituents on Nitrogen Facilitate the Osmium-Catalyzed Asymmetric Aminohydroxylation. *Angew. Chem., Int. Ed. Engl.* **1996**, *35*, 2810−2813.
(29) Bruncko, M.; Schlingloff, G.; Sharpless, K. B. *N*-Bromoacetamide—A New Nitrogen Source for the Catalytic Asymmetric Aminohydroxylation of Olefins. *Angew. Chem., Int. Ed. Engl.* **1997**, *36*, 1483−1486.
(30) Cui, Y.; He, C. Efficient Aziridination of Olefins Catalyzed by a Unique Disilver(I) Compound. *J. Am. Chem. Soc.* **2003**, *125*, 16202−16203.
(31) Lebel, H.; Huard, K.; Lectard, S. N-Tosyloxycarbamates as a Source of Metal Nitrenes: Rhodium-Catalyzed C−H Insertion and Aziridination Reactions. *J. Am. Chem. Soc.* **2005**, *127*, 14198−14199.
(32) Mahoney, J. M.; Smith, C. R.; Johnston, J. N. Brønsted Acid-Promoted Olefin Aziridination and Formal *anti*-Aminohydroxylation. *J. Am. Chem. Soc.* **2005**, *127*, 1354−1355.
(33) Ton, T. M. U.; Tejo, C.; Tiong, D. L. Y.; Chan, P. W. H. Copper(II) Triflate Catalyzed Amination and Aziridination of 2-Alkyl Substituted 1,3-Dicarbonyl Compounds. *J. Am. Chem. Soc.* **2012**, *134*, 7344−7350.
(34) Rigoli, J. W.; Weatherly, C. D.; Alderson, J. M.; Vo, B. T.; Schomaker, J. M. Tunable, Chemoselective Amination via Silver Catalysis. *J. Am. Chem. Soc.* **2013**, *135*, 17238−17241.
(35) Llaveria, J.; Beltrán, Á.; Sameera, W. M. C.; Locati, A.; Díaz-Requejo, M. M.; Matheu, M. I.; Castillón, S.; Maseras, F.; Pérez, P. J. Chemo-, Regio-, and Stereoselective Silver-Catalyzed Aziridination of Dienes: Scope, Mechanistic Studies, and Ring-Opening Reactions. *J. Am. Chem. Soc.* **2014**, *136*, 5342−5350.
(36) Olson, D. E.; Su, J. Y.; Roberts, D. A.; Du Bois, J. Vicinal Diamination of Alkenes under Rh-Catalysis. *J. Am. Chem. Soc.* **2014**, *136*, 13506−13509.
(37) Dolan, N. S.; Scamp, R. J.; Yang, T.; Berry, J. F.; Schomaker, J. M. Catalyst-Controlled and Tunable, Chemoselective Silver-Catalyzed Intermolecular Nitrene Transfer: Experimental and Computational Studies. *J. Am. Chem. Soc.* **2016**, *138*, 14658−14667.
(38) Maestre, L.; Sameera, W. M. C.; Díaz-Requejo, M. M.; Maseras, F.; Pérez, P. J. A General Mechanism for the Copper- and Silver-Catalyzed Olefin Aziridination Reactions: Concomitant Involvement of the Singlet and Triplet Pathways. *J. Am. Chem. Soc.* **2013**, *135*, 1338−1348.
(39) Klotz, K. L.; Slominski, L. M.; Riemer, M. E.; Phillips, J. A.; Halfen, J. A. Mechanism of the Iron-Mediated Alkene Aziridination Reaction: Experimental and Computational Investigations. *Inorg. Chem.* **2009**, *48*, 801−803.
(40) Zdilla, M. J.; Abu-Omar, M. M. Mechanism of Catalytic Aziridination with Manganese Corrole: The Often Postulated High-Valent Mn(V) Imido Is Not the Group Transfer Reagent. *J. Am. Chem. Soc.* **2006**, *128*, 16971−16979.
(41) Tan, Y.; Han, F.; Hemming, M.; Wang, J.; Harms, K.; Xie, X.; Meggers, E. Asymmetric Ring-Closing Aminooxygenation of Alkenes en Route to 2-Amino-1,3-Diols with Vicinal Stereocenters. *Org. Lett.* **2020**, *22*, 6653−6656.
(42) Ju, M.; Weatherly, C. D.; Guzei, I. A.; Schomaker, J. M. Chemo- and Enantioselective Intramolecular Silver-Catalyzed Aziridinations. *Angew. Chem., Int. Ed.* **2017**, *56*, 9944−9948.
(43) Jiang, H.; Lang, K.; Lu, H.; Wojtas, L.; Zhang, X. P. Asymmetric Radical Bicyclization of Allyl Azidoformates via Cobalt(II)-Based Metalloradical Catalysis. *J. Am. Chem. Soc.* **2017**, *139*, 9164−9167.
(44) Donohoe, T. J.; Johnson, P. D.; Cowley, A.; Keenan, M. The Tethered Aminohydroxylation (TA) of Cyclic Allylic Carbamates. *J. Am. Chem. Soc.* **2002**, *124*, 12934−12935.
(45) Donohoe, T. J.; Chughtai, M. J.; Klauber, D. J.; Griffin, D.; Campbell, A. D. *N*-Sulfonyloxy Carbamates as Reoxidants for the Tethered Aminohydroxylation Reaction. *J. Am. Chem. Soc.* **2006**, *128*, 2514−2515.
(46) Donohoe, T. J.; Callens, C. K. A.; Thompson, A. L. Tethered Aminohydroxylation (TA) Reaction of Amides. *Org. Lett.* **2009**, *11*, 2305−2307.
(47) Danielec, H.; Klügge, J.; Schlummer, B.; Bach, T. $FeCl_2$-Catalyzed Intramolecular Chloroamination Reactions. *Synthesis* **2006**, *2006*, 551−556.
(48) Liu, G.-S.; Zhang, Y.-Q.; Yuan, Y.-A.; Xu, H. Iron(II)-Catalyzed Intramolecular Aminohydroxylation of Olefins with Functionalized Hydroxylamines. *J. Am. Chem. Soc.* **2013**, *135*, 3343−3346.

https://dx.doi.org/10.1021/jacs.1c00652
J. Am. Chem. Soc. 2021, 143, 3993−4004

(49) Lu, D.-F.; Liu, G.-S.; Zhu, C.-L.; Yuan, B.; Xu, H. Iron(II)-Catalyzed Intramolecular Olefin Aminofluorination. *Org. Lett.* **2014**, *16*, 2912−2915.
(50) Lu, D.-F.; Zhu, C.-L.; Jia, Z.-X.; Xu, H. Iron(II)-Catalyzed Intermolecular Amino-Oxygenation of Olefins through the N−O Bond Cleavage of Functionalized Hydroxylamines. *J. Am. Chem. Soc.* **2014**, *136*, 13186−13189.
(51) Tian, J.-S.; Zhu, C.-L.; Chen, Y.-R.; Xu, H. Iron-Catalyzed Diastereoselective Intramolecular Olefin Aminobromination with Bromide Ion. *Synthesis* **2015**, *47*, 1709−1715.
(52) Fayssal, S. A.; Giungi, A.; Berhal, F.; Prestat, G. Iron-Catalyzed Intra-intermolecular Aminoazidation of Alkenes. *Org. Process Res. Dev.* **2020**, *24*, 695−703.
(53) Dequirez, G.; Pons, V.; Dauban, P. Nitrene Chemistry in Organic Synthesis: Still in Its. *Angew. Chem., Int. Ed.* **2012**, *51*, 7384−7395.
(54) Jeffrey, J. L.; Sarpong, R. Intramolecular C(sp^3)−H amination. *Chem. Sci.* **2013**, *4*, 4092−4106.
(55) Kluegge, J.; Herdtweck, E.; Bach, T. Iron(II)-Catalyzed Chlorolactamization of γ,δ-Unsaturated Carboxylic Acids. *Synlett* **2004**, *2004*, 1199−1202.
(56) Conway, J. H.; Rovis, T. Regiodivergent Iridium(III)-Catalyzed Diamination of Alkenyl Amides with Secondary Amines: Complementary Access to γ- or δ-Lactams. *J. Am. Chem. Soc.* **2018**, *140*, 135−138.
(57) Dubé, P.; Nathel, N. F. F.; Vetelino, M.; Couturier, M.; Aboussafy, C. L.; Pichette, S.; Jorgensen, M. L.; Hardink, M. Carbonyldiimidazole-Mediated Lossen Rearrangement. *Org. Lett.* **2009**, *11*, 5622−5625.
(58) Li, D.; Wu, T.; Liang, K.; Xia, C. Curtius-like Rearrangement of an Iron−Nitrenoid Complex and Application in Biomimetic Synthesis of Bisindolylmethanes. *Org. Lett.* **2016**, *18*, 2228−2231.
(59) Park, Y.; Park, K. T.; Kim, J. G.; Chang, S. Mechanistic Studies on the Rh(III)-Mediated Amido Transfer Process Leading to Robust C−H Amination with a New Type of Amidating Reagent. *J. Am. Chem. Soc.* **2015**, *137*, 4534−4542.
(60) Shin, K.; Kim, H.; Chang, S. Transition-Metal-Catalyzed C−N Bond Forming Reactions Using Organic Azides as the Nitrogen Source: A Journey for the Mild and Versatile C−H Amination. *Acc. Chem. Res.* **2015**, *48*, 1040−1052.
(61) Hong, S. Y.; Park, Y.; Hwang, Y.; Kim, Y. B.; Baik, M.-H.; Chang, S. Selective formation of γ-lactams via C−H amidation enabled by tailored iridium catalysts. *Science* **2018**, *359*, 1016−1021.
(62) Hong, S. Y.; Son, J.; Kim, D.; Chang, S. Ir(III)-Catalyzed Stereoselective Haloamidation of Alkynes Enabled by Ligand Participation. *J. Am. Chem. Soc.* **2018**, *140*, 12359−12363.
(63) Hong, S. Y.; Chang, S. Stereodefined Access to Lactams via Olefin Difunctionalization: Iridium Nitrenoids as a Motif of LUMO-Controlled Dipoles. *J. Am. Chem. Soc.* **2019**, *141*, 10399−10408.
(64) Hong, S. Y.; Kim, D.; Chang, S. Catalytic access to carbocation intermediates via nitrenoid transfer leading to allylic lactams. *Nat. Catal.* **2021**, *4*, 79−88.
(65) Caruano, J.; Muccioli, G. G.; Robiette, R. Biologically active γ-lactams: synthesis and natural sources. *Org. Biomol. Chem.* **2016**, *14*, 10134−10156.
(66) Lei, H.; Conway, J. H.; Cook, C. C.; Rovis, T. Ligand Controlled Ir-Catalyzed Regiodivergent Oxyamination of Unactivated Alkenes. *J. Am. Chem. Soc.* **2019**, *141*, 11864−11869.
(67) Schley, N. D.; Halbert, S.; Raynaud, C.; Eisenstein, O.; Crabtree, R. H. Symmetrical Hydrogen Bonds in Iridium(III) Alkoxides with Relevance to Outer Sphere Hydrogen Transfer. *Inorg. Chem.* **2012**, *51*, 12313−12323.
(68) Houk, K. N.; Sims, J.; Duke, R. E.; Strozier, R. W.; George, J. K. Frontier Molecular Orbitals of 1,3 Dipoles and Dipolarophiles. *J. Am. Chem. Soc.* **1973**, *95*, 7287−7301.
(69) te Velde, G.; Bickelhaupt, F. M.; Baerends, E. J.; Fonseca Guerra, C.; van Gisbergen, S. J. A.; Snijders, J. G.; Ziegler, T. Chemistry with ADF. *J. Comput. Chem.* **2001**, *22*, 931−967.
(70) Fonseca Guerra, C.; Snijders, J. G.; te Velde, G.; Baerends, E. J. Towards an order-N DFT method. *Theor. Chem. Acc.* **1998**, *99*, 391−403.
(71) Baerends, E. J.; Ellis, D. E.; Ros, P. Self-consistent molecular Hartree—Fock—Slater calculations I. The computational procedure. *Chem. Phys.* **1973**, *2*, 41−51.
(72) Bickelhaupt, F. M.; Houk, K. N. Analyzing Reaction Rates with the Distortion/Interaction-Activation Strain Model. *Angew. Chem., Int. Ed.* **2017**, *56*, 10070−10086.
(73) van Vliet, K. M.; de Bruin, B. Dioxazolones: Stable Substrates for the Catalytic Transfer of Acyl Nitrenes. *ACS Catal.* **2020**, *10*, 4751−4769.
(74) Park, Y.; Jee, S.; Kim, J. G.; Chang, S. Study of Sustainability and Scalability in the Cp*Rh(III)-Catalyzed Direct C−H Amidation with 1,4,2-Dioxazol-5-ones. *Org. Process Res. Dev.* **2015**, *19*, 1024−1029.
(75) On the other hand, when substrates having one more methylene linker between the dioxazolone and double bond were tested, the desired six-membered products were not formed.
(76) Kolb, H. C.; Finn, M. G.; Sharpless, K. B. Click Chemistry: Diverse Chemical Function from a Few Good Reactions. *Angew. Chem., Int. Ed.* **2001**, *40*, 2004−2021.
(77) After completion of the reaction, significant amounts of trimethylsilanol (TMSOH) and 1,1,1,3,3,3-hexamethyldisiloxane (TMS_2O) were detected in the crude reaction mixture by ^{1}H and ^{29}Si NMR analysis to reveal that NFTB or residual water might cooperate with the sulfonyl group to insert $TMSN_3$ into the carbocationic intermediate. See the related reference: Humbrías-Martín, J.; Pérez-Aguilar, M. C.; Mas-Ballesté, R.; Dentoni Litta, A.; Lattanzi, A.; Della Sala, G.; Fernández-Salas, J. A.; Alemán, J. Enantioselective Conjugate Azidation of α,β-Unsaturated Ketones under Bifunctional Organocatalysis by Direct Activation of $TMSN_3$. *Adv. Synth. Catal.* **2019**, *361*, 4790−4796.
(78) In the reaction mixture, trimethylsilanol (TMSOH) and 1,1,1,3,3,3-hexamethyldisiloxane (TMS_2O) were detected in ^{1}H NMR and ^{29}Si NMR spectra.
(79) Of special note, no production of **17** was detected when the preisolated **14** was allowed to react with indole under the standard conditions. suggesting that the *in situ* generation of *threo*-**14** and then conversion to *erythro*-**17** via an S_N2-like process is unlikely.
(80) Chu, S.-f.; Zhang, J.-t. Recent advances in the study of (−)Clausenamide: chemistry, biological activities and mechanism of action. *Acta Pharm. Sin. B* **2014**, *4*, 417−423.
(81) Jang, J.-H.; Asami, Y.; Jang, J.-P.; Kim, S.-O.; Moon, D. O.; Shin, K.-S.; Hashizume, D.; Muroi, M.; Saito, T.; Oh, H.; Kim, B. Y.; Osada, H.; Ahn, J. S. Fusarisetin A, an Acinar Morphogenesis Inhibitor from a Soil Fungus, *Fusarium* sp. FN080326. *J. Am. Chem. Soc.* **2011**, *133*, 6865−6867.
(82) Harris, A. L.; Carmichael, J.; Cantwell, B. M. J.; Dowsett, M. Zoladex: Endocrine and therapeutic effects in post-menopausal breast cancer. *Br. J. Cancer* **1989**, *59*, 97−99.
(83) Fenteany, G.; Standaert, R.; Lane, W.; Choi, S.; Corey, E.; Schreiber, S. Inhibition of Proteasome Activities and Subunit-Specific Amino-Terminal Threonine Modification by Lactacystin. *Science* **1995**, *268*, 726−731.
(84) Dhillon, S. Ivosidenib: First Global Approval. *Drugs* **2018**, *78*, 1509−1516.
(85) Lee, K. L.; Ambler, C. M.; Anderson, D. R.; Boscoe, B. P.; Bree, A. G.; Brodfuehrer, J. I.; Chang, J. S.; Choi, C.; Chung, S.; Curran, K. J.; Day, J. E.; Dehnhardt, C. M.; Dower, K.; Drozda, S. E.; Frisbie, R. K.; Gavrin, L. K.; Goldberg, J. A.; Han, S.; Hegen, M.; Hepworth, D.; Hope, H. R.; Kamtekar, S.; Kilty, I. C.; Lee, A.; Lin, L.-L.; Lovering, F. E.; Lowe, M. D.; Mathias, J. P.; Morgan, H. M.; Murphy, E. A.; Papaioannou, N.; Patny, A.; Pierce, B. S.; Rao, V. R.; Saiah, E.; Samardjiev, I. J.; Samas, B. M.; Shen, M. W. H.; Shin, J. H.; Soutter, H. H.; Strohbach, J. W.; Symanowicz, P. T.; Thomason, J. R.; Trzupek, J. D.; Vargas, R.; Vincent, F.; Yan, J.; Zapf, C. W.; Wright, S. W. Discovery of Clinical Candidate 1-{[(2*S*,3*S*,4*S*)-3-Ethyl-4-fluoro-5-oxopyrrolidin-2-yl]methoxy}-7-methoxyisoquinoline-6-carboxamide

https://dx.doi.org/10.1021/jacs.1c00652
J. Am. Chem. Soc. 2021, 143, 3993−4004

(PF-06650833), a Potent, Selective Inhibitor of Interleukin-1 Receptor Associated Kinase 4 (IRAK4), by Fragment-Based Drug Design. *J. Med. Chem.* **2017**, *60*, 5521−5542.
(86) Jacobi, P. A.; Lee, K. Total Syntheses of (±)- and (−)-Stemoamide. *J. Am. Chem. Soc.* **2000**, *122*, 4295−4303.
(87) Endo, A.; Danishefsky, S. J. Total Synthesis of Salinosporamide A. *J. Am. Chem. Soc.* **2005**, *127*, 8298−8299.
(88) Stapon, A.; Li, R.; Townsend, C. A. Carbapenem Biosynthesis: Confirmation of Stereochemical Assignments and the Role of CarC in the Ring Stereoinversion Process from L-Proline. *J. Am. Chem. Soc.* **2003**, *125*, 8486−8493.
(89) Ma, B.; Banerjee, B.; Litvinov, D. N.; He, L.; Castle, S. L. Total Synthesis of the Antimitotic Bicyclic Peptide Celogentin C. *J. Am. Chem. Soc.* **2010**, *132*, 1159−1171.
(90) Soloshonok, V. A.; Cai, C.; Hruby, V. J. (*S*)- or (*R*)-3-(*E*-Enoyl)-4-phenyl-1,3- oxazolidin-2-ones: Ideal Michael Acceptors To Afford a Virtually Complete Control of Simple and Face Diastereoselectivity in Addition Reactions with Glycine Derivatives. *Org. Lett.* **2000**, *2*, 747−750.
(91) Murata, K.; Ikariya, T.; Noyori, R. New Chiral Rhodium and Iridium Complexes with Chiral Diamine Ligands for Asymmetric Transfer Hydrogenation of Aromatic Ketones. *J. Org. Chem.* **1999**, *64*, 2186−2187.
(92) Park, Y.; Chang, S. Asymmetric formation of γ-lactams via C−H amidation enabled by chiral hydrogen-bond-donor catalysts. *Nat. Catal.* **2019**, *2*, 219−227.
(93) Pendleton, I. M.; Pérez-Temprano, M. H.; Sanford, M. S.; Zimmerman, P. M. Experimental and Computational Assessment of Reactivity and Mechanism in C(sp^3)−N Bond-Forming Reductive Elimination from Palladium(IV). *J. Am. Chem. Soc.* **2016**, *138*, 6049−6060.
(94) Planas, O.; Wang, F.; Leutzsch, M.; Cornella, J. Fluorination of arylboronic esters enabled by bismuth redox catalysis. *Science* **2020**, *367*, 313−317.
(95) Wang, H.; Park, Y.; Bai, Z.; Chang, S.; He, G.; Chen, G. Iridium-Catalyzed Enantioselective C(sp3)−H Amidation Controlled by Attractive Noncovalent Interactions. *J. Am. Chem. Soc.* **2019**, *141*, 7194−7201.

https://dx.doi.org/10.1021/jacs.1c00652
J. Am. Chem. Soc. 2021, 143, 3993−4004